Physica A 569 (2021) 125753

Contents lists available at ScienceDirect

Physica A

journal homepage: www.elsevier.com/locate/physa

Coherence-enhanced thermal amplification for small systems

Shanhe Su [a,*], Yanchao Zhang [b], Bjarne Andresen [c], Jincan Chen [a]

[a] Department of Physics, Xiamen University, Xiamen 361005, China
[b] School of Science, Guangxi University of Science and Technology, Liuzhou, 545006, China
[c] Niels Bohr Institute, University of Copenhagen, Universitetsparken 5, DK-2100 Copenhagen Ø, Denmark

ARTICLE INFO

Article history:
Received 8 September 2019
Received in revised form 2 November 2020
Available online 11 January 2021

Keywords:
Quantum coherence
Three-level system
Thermal amplification
Thermal conductance

ABSTRACT

Coherent control of self-contained quantum systems offers the possibility to fabricate smallest thermal transistors. The steady coherence created by the delocalization of electronic excited states arouses nonlinear heat transports in non-equilibrium environment. Applying this result to a three-level quantum system, we show that quantum coherence gives rise to negative differential thermal resistances, making the thermal transistor suitable for thermal amplification. The results demonstrate that quantum coherence facilitates efficient thermal signal processing and can open a new field in the application of quantum thermal management devices.

1. Introduction

A thermal transistor, like its electronic counterpart, is capable of implementing heat flux switching and modulating. The effects of negative differential thermal resistance (NDTR) play a key role in the development of thermal transistors [1–6]. Classical dynamic descriptions utilizing Frenkel–Kontorova lattices conclude that nonlinear lattices are the origin of NDTR [7–11]. Ben-Abdallah et al. introduced a distinct type of thermal transistors based on the radiative heat transfer of thermal photons between two bodies [12–15]. Joulain et al. first proposed a quantum thermal transistor with strong coupling between the interacting spins, where the competition between different decay channels makes the temperature dependence of the base flux slow enough to obtain a high amplification [16]. Zhang et al. predicted that asymmetric Coulomb blockade in quantum-dot thermal transistors would result in a NDTR [17]. Stochastic fluctuations in mesoscopic systems have been regarded as an alternate resource for the fast switching of heat flows [18].

Recent studies showed that quantum coherence exhibits the ability to enhance the efficiency of thermal converters, such as quantum heat engines [19–21] and artificial light-harvesting systems [22,23]. Interference between multiple transitions in nonequilibrium environments enables us to generate non-vanishing steady quantum coherence [24,25]. Evidence is growing that long-lived coherence boosts the transport of energy from light-harvesting antennas to photosynthetic reaction centers [26,27]. The question arises whether quantum interference and coherence effects could also induce nonlinear heat conduction and enhance the performance of a thermal transistor.

Scovil and Schulz-DuBois originally proposed a three-level maser system as an example of a Carnot engine and applied detailed balance ideas to obtain the maser efficiency formula [28]. Because the controlled (output) thermal flux is normally higher than the controlling (input) thermal flux, a thermal transistor is able to amplify or switch a small signal. The amplification factor must be tailored to suit specific situations. The Scovil and Schulz-DuBois maser model is not applicable for fabricating thermal transistors, owing to the fact that its amplification factor is simply a constant defined by the

* Corresponding author.
E-mail addresses: sushanhe@xmu.edu.cn (S. Su), jcchen@xmu.edu.cn (J. Chen).

https://doi.org/10.1016/j.physa.2021.125753
0378-4371/

maser frequency relative to the pump frequency [29,30]. However, the coherent excitation-energy transfer created by the delocalization of electronic excited states may aid in the design of powerful thermal devices. Coherent control of a three-level system (TLS) provides us a heuristic approach to better understand the prime requirements for the occurrence of anomalous thermal conduction in quantum systems.

In this paper, we design a quantum thermal transistor consisting of a TLS coupled to three separate baths. The dynamics of the system is derived by considering the coupling between the two excited states. Steady-state solutions will be used to prove that the coherent transitions between the two excited states induce nonlinearity in nonequilibrium quantum systems. Further analysis shows that quantum coherence gives rise to a NDTR and helps improve the thermal amplification.

2. Model and principles

2.1. The three-level system (TLS)

Fig. 1 shows the TLS modeled by the Hamiltonian H_S as

$$H_S = \sum_{i=0,1,2} \varepsilon_i |i\rangle \langle i| + \Delta(|1\rangle \langle 2| + |2\rangle \langle 1|), \tag{1}$$

where ε_1 (ε_2) gives the energy level of the excited states in the molecules $|1\rangle$ ($|2\rangle$), ε_0 denotes the energy of the ground state $|0\rangle$ and is set to zero, and Δ describes the excitonic coupling between states $|1\rangle$ and $|2\rangle$. For the models of biological light reactions, Δ occurs naturally as a consequence of the intermolecular forces between two proximal optical dipoles [23,31]. In the presence of the dipole–dipole interaction, the optically excited states become coherently delocalized. $|+\rangle = \cos\theta\,|1\rangle + \sin\theta\,|2\rangle$ and $|-\rangle = \sin\theta\,|1\rangle - \cos\theta\,|2\rangle$ are the usual eigenstates diagonalizing the subspace spanned by $|1\rangle$ and $|2\rangle$ with $\tan 2\theta = 2\Delta/(\varepsilon_1 - \varepsilon_2)$.

The absorption of a photon from the emitter (E) causes an excitation transfer from the ground state $|0\rangle$ to the state $|1\rangle$, whereas phonons are emitted into the base (B) by the transitions between $|1\rangle$ and $|2\rangle$. The cycle is closed by the transition between $|2\rangle$ and $|0\rangle$, and the rest of the energy is released as a photon to the collector (C). The Hamiltonians of the emitter, collector, and base are $H_i = \sum_k \omega_{ik} a_{ik}^\dagger a_{ik}$ ($i = E$, C, and B), where $a_{ik}^\dagger$ (a_{ik}) refers to the creation (annihilation) operator of the bath mode ω_{ik}. The TLS couples to the emitter and the collector, each constituted of harmonic oscillators, via coupling constants g_{Ek} and g_{Ck} in the rotating wave approximation, where the corresponding Hamiltonians are formally written as $H_{SE} = \sum_k \left(g_{Ek}^\dagger a_{Ek} |0\rangle \langle 1| + h.c.\right)$ and $H_{SC} = \sum_k \left(g_{Ck}^\dagger a_{Ck} |0\rangle \langle 2| + h.c.\right)$, respectively. The output of the Scovil–Schulz-DuBois maser is a radiation field with a particular frequency, provided there is population inversion between levels ε_1 and ε_2. In this study, the two excited states are coupled with a thermal reservoir, namely, the base. The interaction Hamiltonian of the system with the base is described by

$$H_{SB} = (|1\rangle \langle 1| - |2\rangle \langle 2|) \sum_k g_{Bk} \left(a_{Bk} + a_{Bk}^\dagger\right). \tag{2}$$

For a finite coupling Δ, the base modeled by Eq. (2) induces not only decoherence but also relaxation [32]. Here, we consider that the excited states are coupled to the base via diagonal interaction, which describes, for instance, the interaction between a localized crystal defect and the lattice phonons field [33]. This type of the system-bath interaction has been widely applied in studying the processes of phonon-assisted excitation transfer [34,35], nonequilibrium energy transfer [36], and photosynthesis [37]. The base behaves like a pure-dephasing reservoir acting on the quantum system. Eq. (A.4) in Appendix A will prove that the coherence described by the off-diagonal element of the density matrix of the system is closely related to the dephasing rate. In Fig. 5, we show that the increase of the dephasing rate induces the loss of steady coherence. Transport of thermal energy between the system and the base emerges with the help of the excitonic coupling Δ. The counterintuitive effect of the energy exchange between the two excited states and the dephasing bath becomes evident when the system operator coupled to the base is replaced by

$$\begin{aligned} |1\rangle \langle 1| = {} & \cos\theta\cos\theta\,|+\rangle \langle +| + \sin\theta\sin\theta\,|-\rangle \langle -| \\ & + \sin\theta\cos\theta\,(|+\rangle \langle -| + |-\rangle \langle +|) \end{aligned} \tag{3}$$

and

$$\begin{aligned} |2\rangle \langle 2| = {} & \sin\theta\sin\theta\,|+\rangle \langle +| + \cos\theta\cos\theta\,|-\rangle \langle -| \\ & - \cos\theta\sin\theta\,(|+\rangle \langle -| + |-\rangle \langle +|). \end{aligned} \tag{4}$$

The first two operators in $|1\rangle \langle 1|$ and $|2\rangle \langle 2|$ describe the pure dephasing of a two-level system, whereas the third term leads to the energy exchange between the system and the base with an effective coupling proportional to the product $\sin\theta\cos\theta$, i.e.,

$$H_{SB-eff} = 2\sin\theta\cos\theta\,(|+\rangle \langle -| + |-\rangle \langle +|) \sum_k g_k \left(a_k + a_k^\dagger\right). \tag{5}$$

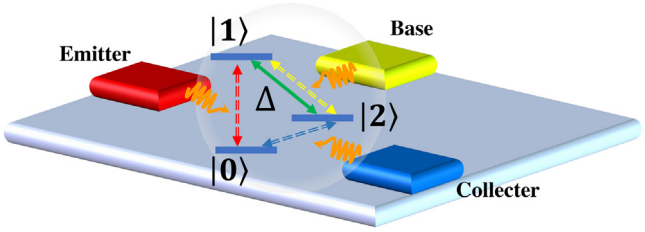

Fig. 1. Schematic illustration of the quantum thermal transistor composed of a three-level system (TLS) interacting with three baths: its ground state $|0\rangle$ and excited state $|1\rangle$ ($|2\rangle$) are coupled with the emitter (collector); the excited states $|1\rangle$ and $|2\rangle$ are diagonal-coupled with the base; and the coupling strength between $|1\rangle$ and $|2\rangle$ is characterized by Δ.

In reality, the TLS can be realized in the photosynthesis process. The pumping light, taking the sunlight photons for example, is considered as the high temperature emitter. The collector is formed by the surrounding electromagnetic environment which models the energy transfer to the reaction center. The base provides the phonon modes coupled with the excited states [30,38].

2.2. Evolution equation for the density operator of the TLS

The TLS becomes irreversible due to the interaction with its surrounding environment. In the following derivation, the interactions H_{SE}, H_{SC}, and H_{SB} are considered to be weak enough such that the thermal states of the baths are unaffected by the TLS. Using the Born–Markov approximation, which involves the assumptions that the environment is time independent and the environment correlations decay rapidly in comparison to the typical time scale of the system evolution [39], we get the quantum dynamics of the system in $\hbar = 1$ units, i.e.,

$$\frac{d\rho}{dt} = -i[H_S, \rho] + \mathcal{D}_E[\rho] + \mathcal{D}_B[\rho] + \mathcal{D}_C[\rho]. \tag{6}$$

The operators $\mathcal{D}_i[\rho]$ ($i = E, B,$ and C) denote the dissipative Lindblad superoperators associated with the emitter, base, and collector (Appendix A, Eq. (A.1)), which take the form

$$\mathcal{D}_i[\rho] = \sum_v \gamma_i(v)\left[A_i(v)\,\rho A_i^\dagger(v) - \frac{1}{2}\left\{\rho, A_i^\dagger(v)\,A_i(v)\right\}\right], \tag{7}$$

where $v = \varepsilon - \varepsilon'$ is the energy difference between the two arbitrary eigenvalues of H_S, and $A_i(v)$ is the jump operator associated with the interaction between the system and bath i. Considering a quantum bath consisting of harmonic oscillators, we have the decay rate $\gamma_i(v) = \Gamma_i(v)\,n_i(v)$ for $v < 0$ and $\gamma_i(v) = \Gamma_i(v)[1 + n_i(v)]$ for $v > 0$, where $\Gamma_i(v)$ labels the decoherence rate and is related to the spectral density of the bath, and T_i is the temperature of bath i. The thermal occupation number in a mode is written as $n_i(v) = 1/\left[e^{v/(k_B T_i)} - 1\right]$. The Boltzmann constant k_B is set to unity in the following.

2.3. Coherence induced nonlinearity and thermal transistor effects

The steady-state populations and coherence of the open quantum system are obtained by setting the left-hand side of Eq. (6) equal zero. Then the steady state energy fluxes are determined by the average energy going through the TLS, i.e.,

$$\dot{E}(\infty) = \sum_{i=E,C,B} \mathrm{Tr}\{H_S \mathcal{D}_i[\rho(\infty)]\} = J_E + J_C + J_B = 0, \tag{8}$$

which complies with the 1st law of thermodynamics. The heat fluxes J_E, J_C, and J_B are defined with respect to their own dissipative operators. Thus,

$$\begin{aligned} J_E &= -\Gamma_E(\varepsilon_1)(n_E + 1)\left[\varepsilon_1\left(\rho_1 - \frac{n_E}{n_E + 1}\rho_0\right) + \Delta\Re(\rho_{12})\right] \\ &= J_{E1} + J_{E2}, \end{aligned} \tag{9}$$

$$\begin{aligned} J_C &= -\Gamma_C(\varepsilon_2)(n_C + 1)\left[\varepsilon_2\left(\rho_2 - \frac{n_C}{n_C + 1}\rho_0\right) + \Delta\Re(\rho_{12})\right] \\ &= J_{C1} + J_{C2}, \end{aligned} \tag{10}$$

and

$$J_B = -\Gamma_B(\omega)\sin^2 2\theta(2n_B+1)\Big[\frac{\varepsilon_1-\varepsilon_2}{2}(\rho_1-\rho_2) + \frac{\sqrt{(\varepsilon_1-\varepsilon_2)^2/4+\Delta^2}}{2n_B+1} + 2\Delta\Re(\rho_{12})\Big] = J_{B1}+J_{B2}. \tag{11}$$

The three heat fluxes are no longer linear functions of the rate of the spontaneous emission, indicating that the symmetric property is closely related to the base induced coherence of the excited states. In Eqs. (9)–(11), each heat flux is divided into two categories. The terms J_{i2} $(i = E, C, B)$ are connected to the coherence in the local basis, i.e., $\Re(\rho_{12})$ (the real part of ρ_{12}). J_{i1} is the remainder components depending on the populations of the TLS.

The thermodynamics of a TLS was originally proposed by Scovil and Schulz-DuBois [28]. Boukobza et al. obtained the Scovil–Schulz-DuBois maser efficiency formula when the TLS was operated as an amplifier [29,40,41]. The efficiency of the amplifier is defined as the ratio of the output energy to the energy extracted from the hot reservoir [42]. In a nonequilibrium steady state, the efficiency is a fixed value which equals $1-(\varepsilon_2-\varepsilon_0)/(\varepsilon_1-\varepsilon_0)$, because all heat fluxes are linear functions of the same rate of excitation. However, a thermal transistor is a thermal device used to amplify or switch the thermal currents at the collector and the emitter via a small change in the base heat flux or the base temperature. Nonlinearity is the essential element needed to give rise to such thermal amplification. For the purpose of flexible control of the thermal currents, the characteristic functions of the TLS should not entirely depend upon the energy level structure of the TLS.

A thermal amplifier requires a transistor with a high amplification factor $\alpha_{E/C}$, which is defined as the instantaneous rate of change of the emitter or collector heat flux to the heat flux applied at the base. The quantum thermal transistor has fixed emitter and collector temperatures T_E and T_C $(T_E > T_C)$, respectively. The fluxes J_E and J_C are controlled by J_B, which can be adjusted by the base temperature T_B. Then the amplification factor $\alpha_{E/C}$ explicitly reads

$$\alpha_{E/C} = \frac{\partial J_{E/C}}{\partial J_B}. \tag{12}$$

The ratio of the slopes of the thermal currents is the key parameter to find out whether the amplification effect exists. When $|\alpha_{E/C}| > 1$, a small change in J_B stimulates a large variation in J_E or J_C and the thermal transistor effect appears. This implies that a small change of the heat flux signal of the base would lead to noticeable changes of the energy flowing through the emitter and collector.

We consider heat fluxes from the baths into the TLS as positive. As T_E and T_C are fixed values and T_B is adjustable, the thermal conductances of the three terminals are defined as

$$\sigma_i = -\frac{\partial J_i}{\partial T_B} = \sigma_{i1}+\sigma_{i2}, \tag{13}$$

where $\sigma_{ij} = -\frac{\partial J_{ij}}{\partial T_B}$ $(i = E, C, B; j = 1, 2)$, σ_{i1} are the thermal conductances with respect to the spontaneous emission, and σ_{i2} are the thermal conductances relying on the coherence $\Re(\rho_{12})$. The energy conservation in Eq. (8) implies the relationship of the three thermal conductances, $\sigma_B+\sigma_C+\sigma_E = 0$. Using Eq. (13), the amplification factor in Eq. (12) can be recast in terms of σ_E and σ_C, i.e.,

$$\alpha_{E/C} = \frac{\sigma_{E/C}}{\sigma_B} = -\frac{\sigma_{E/C}}{\sigma_C+\sigma_E}. \tag{14}$$

The absolute value of the amplification factor $|\alpha_{E/C}| > 1$ implies that one of the thermal conductances is negative, i.e., $\sigma_C < 0$ or $\sigma_E < 0$. This means that there exists a NDTR, and consequently, the TLS can behave as a thermal transistor by controlling the heat flow in analogy to the usual electric transistor.

3. Results and discussion

In the following section, we need to explore the extent to which the quantum nature of the TLS affects the thermal transistor. The formalism obtained here will allow us to access how coherences can lead to a NDTR and an enhancement of the amplification factor. To do so, the thermal conductances and temperatures of the three baths are recast in units of Δ. In the wide-band approximation, we write the decoherence rates of the three terminals as $\Gamma_i(v) = \Gamma_i$ and the dephasing rate of the base as $\gamma_B(0) = \gamma_0$.

Fig. 2(a) shows the thermal conductances σ_i of each terminal as functions of the base temperature T_B. $|\sigma_E|$, σ_C, and σ_B decrease with T_B at low temperature and become constant as T_B approaches T_E. One of the thermal conductances is negative, i.e., $\sigma_E < 0$, satisfying the basis condition for the thermal amplification. In addition, σ_B remains lower than $|\sigma_E|$ and σ_C over the whole range. According to the definitions of thermal conductances in Eq. (13), this phenomenon means that a small difference of the base heat flux J_B due to the change of temperature T_B is able to dramatically change the emitter and collector thermal flows J_E and J_C, leading to a noticeable amplification effect. When T_B is between 100Δ and 200Δ, the variations of $|\sigma_E|$ and σ_C with T_B will be more obvious than that of σ_B. By following the decomposition of the thermal fluxes [Eqs. (9)–(11)], each thermal conductance can be divided into two separate parts [Eq. (13)]. Fig. 2(b)

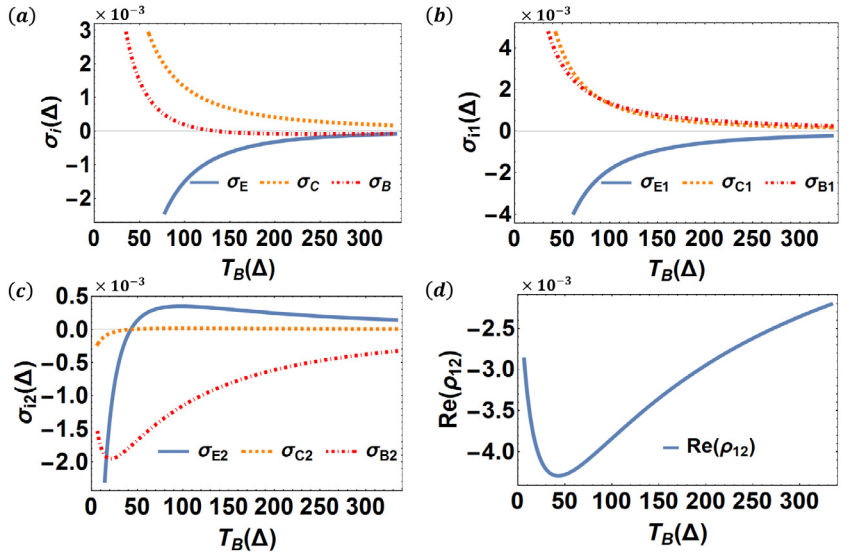

Fig. 2. (a) The overall thermal conductances σ_i; (b) the thermal conductances σ_{i1}; (c) the thermal conductances σ_{i2}; and (d) the real part of the coherence $\Re[\rho_{12}]$ versus the base temperature T_B. We choose the parameters in units of Δ: $\Gamma_E/\Delta = \Gamma_C/\Delta = \Gamma_B/\Delta = \gamma_0/\Delta \equiv 1$, $\varepsilon_1/\Delta = 10$, $\varepsilon_2/\Delta = 7$, $T_E = \Delta/0.003$, and $T_C = \Delta/0.15$.

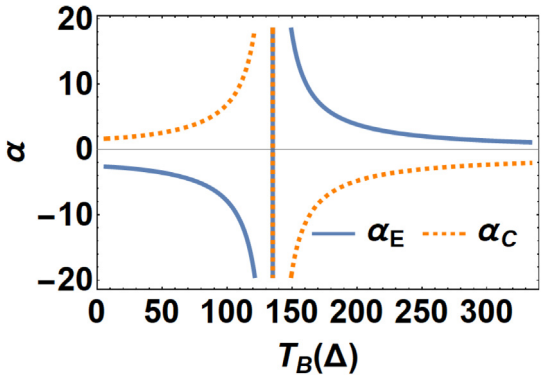

Fig. 3. The amplification factors α_E (solid line) and α_C (dashed line) versus the base temperature T_B. All parameters are the same as those used in Fig. 2.

and (c) display the thermal conductances σ_{i1} pertaining to the population distributions and to the coherence contributed thermal conductances σ_{i2} varying with the base temperature T_B. σ_{E1}, σ_{C1}, and σ_{B1} share a magnitude close to each other, indicating that it is unlikely to create an autonomous thermal amplifier without coherence. Quantum coherence $\Re(\rho_{12})$ exists [Fig. 2(d)], allowing us to modify the thermodynamic behavior through the quantum control. For the two thermal conductances σ_{B1} and σ_{B2} of the base, $\sigma_{B1}>0$ [Fig. 2(b)], whereas σ_{B2} originating from the coherence is negative [Fig. 2(c)], ensuring that we achieve a vanishing σ_B [Fig. 2(a)]. When σ_B approaches zero, Eq. (14) has indicated that one can design a quantum thermal transistor with large amplification factors.

The curves of the amplification factors α_E and α_C as functions of the base temperature T_B are illustrated in Fig. 3. The amplification factors α_E and α_C are clearly greater than 1 over a large range of T_B. As seen from Eq. (14) and Fig. 2, these effects result from $\sigma_E < 0$, which is similar to the property of some electrical circuits and devices where an increase in voltage across the overall assembly results in a decline in electric current through it, i.e., negative differential conductance. Specifically, Fig. 3 shows that the amplification factors diverge at $T_B = 135.3\Delta$ due to the fact that the thermal conductance of the base $\sigma_B = 0$, induced by the quantum coherence. Under these conditions, an infinitesimal change in J_B makes a considerable difference in J_E and J_C. The results demonstrate that there is no fundamental difficulty in constructing small, self-contained thermal amplifiers by using the three-level model, because it is possible to build the steady-state coherence under the nonequilibrium environment. The quantum coherence arouses nonlinear heat transports and gives rise to NDTR, which makes the thermal device suitable for thermal amplification. Despite the dimension of the thermodynamic machines being small, it is still able to operate at a high amplification factor.

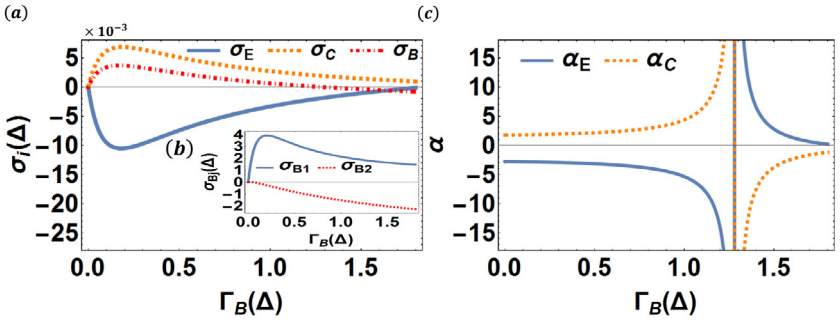

Fig. 4. (a) The overall thermal conductances σ_i; (b) the thermal conductances of the base σ_{Bj} (inset); and (c) the amplification factors α_E (solid line) and α_C (dashed line) versus the decoherence rate of the base Γ_B.

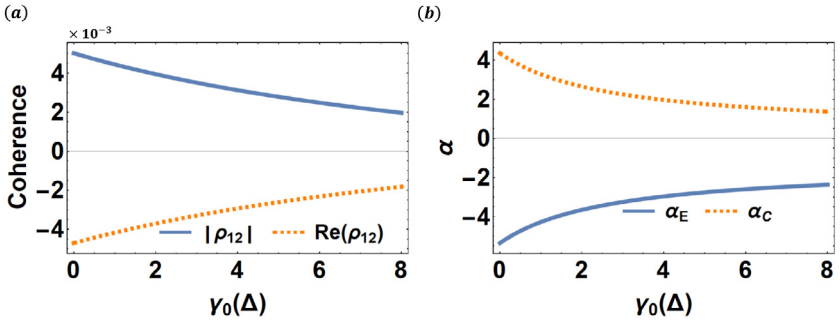

Fig. 5. (a) The absolute value and the real part of coherence, $|\rho_{12}|$ and $\Re[\rho_{12}]$, versus the dephasing rate of the base γ_0. (b) The amplification factors α_E (solid line) and α_C (dashed line) versus the dephasing rate of the base γ_0.

Figs. 4 and 5 reveal the influences of the decoherence rate Γ_B and the dephasing rate of the base γ_0 on the performance of the thermal transistor. The base temperature $T_B = \Delta/0.015$, while the values of other parameters are the same as those used in Fig. 2. The amplification factor α_C increases as Γ_B increases in the small-Γ_B regime ($\Gamma_B < 1.287\Delta$), but the absolute value of α_C decreases as Γ_B increases in the large-Γ_B regime ($\Gamma_B > 1.287\Delta$), while α_C tends to divergence for $\Gamma_B \to 1.287\Delta$. The amplification factor α_E as a function of Γ_B has opposite signs. The decoherence rate Γ_B is an important parameter for building a desirable amplifier. As illustrated in Fig. 4(b), the thermal conductance σ_B of the base is the sum of σ_{B1} and σ_{B2}. Once again, we observe that σ_{B1} is always positive, while the thermal conductance relevant to the coherence effect σ_{B2}<0 leading to a cancellation of the sum when $\Gamma_B \to 1.287\Delta$. For the same reason, the amplification factors diverge at $\Gamma_B \to 1.287\Delta$ when $\sigma_B = 0$.

Coherence is maintained in a nonequilibrium steady state even in the presence of the dephasing bath. However, a large dephasing rate has a deleterious effect on the characteristics of the TLS thermal transistor [Fig. 5(b)]. Fig. 5(a) shows that the absolute value $|\rho_{12}|$ and the real part $\Re[\rho_{12}]$ of coherence are monotonically decreasing functions of γ_0, the decoherence rate of the base. The pure-dephasing bath acting on the TLS induces the loss of steady coherence, yielding smaller $\alpha_{E/C}$.

4. Conclusions

In summary, we proposed a TLS to analyze the effects of the dipole–dipole interaction and the dephasing on the energy transfer processes in a thermal transistor. The coupling between the two excited states of the TLS is capable of generating steady coherence in a nonequilibrium environment, making the thermal fluxes behave nonlinearly. The coherence, at the same time, gives rise to NTDR of the base. Quantum coherence enables the thermal flow through the collector and emitter to be controlled by the temperature of the base. Such a thermal transistor can amplify a small input signal as well as direct heat to flow preferentially in one direction. The thermal transistor effect can be significantly improved by adjusting the base temperature and coherence rate or reducing the dephasing rate.

CRediT authorship contribution statement

Shanhe Su: Conceptualization, Methodology, Software. **Yanchao Zhang:** Software. **Bjarne Andresen:** Writing - reviewing and editing, Supervision. **Jincan Chen:** Writing - reviewing and editing, Supervision.

Declaration of competing interest

The authors declare that they have no known competing financial interests or personal relationships that could have appeared to influence the work reported in this paper.

Acknowledgments

We thank Dr. Dazhi Xu for helpful discussions. This work has been supported by the National Natural Science Foundation of China (Grant No. 11805159), Natural Science Foundation of Fujian Province, China (No. 2019J05003), and Fundamental Research Fund for the Central Universities, China (No. 20720180011).

Appendix A. The dissipative operators of the TLS

The master equation [Eq. (6)] can be derived by using the weak coupling, Markovian, and Weiskopf–Wigner approximations [43–45]. Owing to the weak coupling between the TLS and the baths and setting Δ to be small, the dissipative superoperators of the emitter and collector $\mathcal{D}_E[\rho]$ and $\mathcal{D}_C[\rho]$ are described by the local Liouville operator of the Lindblad form [29,30,43]

$$\begin{aligned}\mathcal{D}_i[\rho] = \Gamma_i(\varepsilon_i)[(n_i+1)\left(O_i^-\rho O_i^+ - \frac{1}{2}\left\{O_i^+O_i^-,\rho\right\}\right) \\ + n_i\left(O_i^+\rho O_i^- - \frac{1}{2}\left\{O_i^-O_i^+,\rho\right\}\right)],\end{aligned} \tag{A.1}$$

where the system operators are defined as $O_E^+ = |1\rangle\langle 0|$, and $O_C^+ = |2\rangle\langle 0|$.

The system-base coupling relates only to the states $|1\rangle$ and $|2\rangle$. It is appropriate to consider the role of the two excited states first, and then the resulting dissipative operator $\mathcal{D}_B[\rho]$ could be readily be incorporated into the dynamics of the TLS. The jump operator associated with the base can be obtained by decomposing the system operators from the system-base interaction Hamiltonian, which is defined as

$$A_B(v) = \sum_{v=\varepsilon-\varepsilon'}\prod_{\varepsilon'}(|1\rangle\langle 1| - |2\rangle\langle 2|)\prod_{\varepsilon}, \tag{A.2}$$

where $\prod_{\varepsilon_\pm} = |\pm\rangle\langle\pm|$ is the projection onto the eigenspace belonging to the optically excited states. The operator $A_B(0) = \cos 2\theta\,(|+\rangle\langle+| - |-\rangle\langle-|)$ describes the dephasing effects due to the interaction with the base, while $A_B(\omega) = \sin 2\theta\,|-\rangle\langle+|$ and $A_B^\dagger(-\omega) = A_B(\omega)$ are related to the decay channels with nonzero transition frequencies. In our case, the sum is extended over $v = 0, \pm\omega$, where $\omega = \varepsilon_+ - \varepsilon_- = \sqrt{(\varepsilon_1-\varepsilon_2)^2 + 4\Delta^2}$. The second-order perturbation method developed for the Lindblad master equation assumes that the interactions between the TLS and the baths are weak, but it is applicable over a broad range of Δ [32]. However, because we use local Liouville operators for describing the dissipations to the emitter and collector, Δ can only be a small value. Putting Eq. (A.2) back into Eq. (7) yields

$$\begin{aligned}\mathcal{D}_B[\rho] = \gamma_B(0)\cos^2 2\theta\left[\tau_z\rho\tau_z^\dagger - \frac{1}{2}\left\{\tau_z^\dagger\tau_z,\rho\right\}\right] \\ + \Gamma_B(\omega)\sin^2 2\theta[(n_B+1)\left(\tau^-\rho\tau^+ - \frac{1}{2}\left\{\tau^+\tau^-,\rho\right\}\right) \\ + n_B\left(\tau^+\rho\tau^- - \frac{1}{2}\left\{\tau^-\tau^+,\rho\right\}\right)].\end{aligned} \tag{A.3}$$

It appears as a surprise to uncover that the dipole–dipole coupling between states $|1\rangle$ and $|2\rangle$ arouses dephasing in this model, where $\gamma_B(0) = \lim_{v\to 0}\gamma_B(v) = \lim_{v\to 0}\frac{\Gamma_B(v)}{v}k_BT_B$ is the dephasing rate due to the base. The dephasing rate is an important effect in molecular and atomic spectroscopy and mesoscopic devices [46–48]. A new set of Pauli operators $\tau_z = |+\rangle\langle+| - |-\rangle\langle-|$, $\tau^+ = |+\rangle\langle-|$, and $\tau^- = |-\rangle\langle+|$ are defined. Eq. (A.3) provides the evidence of the influence of the coupling between states $|1\rangle$ and $|2\rangle$, as indicated in the terms of $\sin^2 2\theta$ and $\cos^2 2\theta$. For purposes of testing on the properties of the entire TLS with all the weakly coupled photon baths, Eq. (A.3) should be transformed back into the local basis utilizing the optical Bloch equations. For the dissipative process of a two level system, the relations of the optical Bloch equations between the bare and dressed pictures are given in Appendix B. Note that $\mathcal{D}_B[\rho]$ is described with the projection on the delocalized state ($|+\rangle$ and $|-\rangle$), while $\mathcal{D}_E[\rho]$ and $\mathcal{D}_C[\rho]$ are written with the original states ($|1\rangle$ and $|2\rangle$). This treatment has been widely adopted in the studies of three-level systems [30,49–51]. A more rigorous calculation requires us to write all the dissipative operators in the dressed-state basis, which is an important topic in need of further research.

According to Eqs. (6), (A.1), and (A.3), we have a coupled set of equations describing the dynamics of the populations, $\rho_i = \langle i|\rho|i\rangle$, and the coherence, $\rho_{ij} = \langle i|\rho|j\rangle$, as follows,

$$\frac{d}{dt}\begin{pmatrix}\rho_{11}-\rho_{22}\\ \rho_{11}+\rho_{22}\\ \Re\left[\rho_{12}\right]\\ \Im\left[\rho_{12}\right]\end{pmatrix} = -M\begin{pmatrix}\rho_{11}-\rho_{22}\\ \rho_{11}+\rho_{22}\\ \Re\left[\rho_{12}\right]\\ \Im\left[\rho_{12}\right]\end{pmatrix} + \begin{pmatrix}\Gamma_E\left(\varepsilon_1\right)n_E-\Gamma_C\left(\varepsilon_2\right)n_C-\Gamma\sin^2 2\theta\cos 2\theta\\ \Gamma_E\left(\varepsilon_1\right)n_E+\Gamma_C\left(\varepsilon_2\right)n_C\\ -\frac{1}{2}\Gamma\sin^3 2\theta\\ 0\end{pmatrix}, \tag{A.4}$$

where the matrix M is shown in Appendix C. For the TLS, the ground state population ρ_{00} should be included and the population conservation becomes $\rho_{00}+\rho_{11}+\rho_{22}=1$. The equations for the off-diagonal terms ρ_{01} and ρ_{02} are absent from Eq. (A.4) and do not affect the steady-state solution. However, the time evolutions of the populations are not decoupled from that of the off-diagonal elements ρ_{12}. $\Re\left[\rho_{12}\right]$ and $\Im\left[\rho_{12}\right]$ are the real and imaginary parts of ρ_{12}, and may not vanish even in the steady state after long time evolution. Specifically, we will find that the coherent transitions between the two excited states induce nonlinearity in the system. The heat fluxes in Eqs. (9)–(11) can be computed based on the steady solution of Eq. (A.4).

Appendix B. The dissipative process of a two level system

The system-base coupling relates only to the excited states $|1\rangle$ and $|2\rangle$. In order to obtain the dynamics of the TLS [Eq. (A.4)], it is convenient to consider the dissipative process of a two-level system first. The two-site Hamiltonian is

$$H_0 = \varepsilon_1|1\rangle\langle 1| + \varepsilon_2|2\rangle\langle 2| + \Delta(|1\rangle\langle 2| + |2\rangle\langle 1|). \tag{B.1}$$

The eigenvalues of H_0 are $\varepsilon_\pm = \left(\varepsilon_1+\varepsilon_2\right)/2 \pm \sqrt{\left(\varepsilon_1-\varepsilon_2\right)^2/4+\Delta^2}$ and the corresponding eigenstates are $|+\rangle$ and $|-\rangle$ as described in the main text.

Based on the interaction Hamiltonian Eq. (B.1) and the dissipative superoperators Eq. (A.3) of the base , we obtain the evolution of the density matrix elements of a two-level system as

$$\dot{\rho}_{++} = -\gamma_B(\omega)\sin^2 2\theta\rho_{++} + \gamma_B(-\omega)\sin^2 2\theta\rho_{--}, \tag{B.2}$$

$$\dot{\rho}_{+-} = -[2\gamma_B(0)\cos^2 2\theta + \frac{1}{2}\Gamma_B(\omega)\sin^2 2\theta\left(2n_B+1\right) + i\omega]\rho_{+-}. \tag{B.3}$$

An alternative solution representation to the optical master equation is provided by the Bloch equations. Since $\langle\tau_z(t)\rangle = tr\left[\tau_z(t)\rho(t)\right] = \rho_{++}-\rho_{--}$, $\langle\tau_+(t)\rangle = tr\left[\tau_+(t)\rho(t)\right] = \rho_{-+}$, $\langle\tau_-(t)\rangle = tr\left[\tau_-(t)\rho(t)\right] = \rho_{+-}$, and $\rho_{++}(t)+\rho_{--}(t)=1$, Eqs. (B.2) and (B.3) can be rewritten as the differential equations of the Bloch vectors

$$\langle\dot{\tau}_z\rangle = -\Gamma_B(\omega)\sin^2 2\theta\left[\left(2n_B+1\right)\langle\tau_z(t)\rangle+1\right], \tag{B.4}$$

$$\langle\dot{\tau}_+\rangle = -[2\gamma_B(0)\cos^2 2\theta + \frac{1}{2}\Gamma_B(\omega)\sin^2 2\theta\left(2n_B+1\right) - i\omega]\langle\tau_+(t)\rangle. \tag{B.5}$$

To transform back into the local basis, we express the elements of the reduced density matrix by the average of the Pauli operators $\left\langle\tau_{z,\pm}\right\rangle_t = tr\left[\tau_{z,\pm}\rho(t)\right]$ and $\left\langle\sigma_{z,\pm}\right\rangle_t = tr\left[\sigma_{z,\pm}\rho(t)\right]$. Together with the relations between the bare and dressed states, it is straightforwardly to obtain

$$\langle\sigma_z(t)\rangle = \cos 2\theta\langle\tau_z(t)\rangle + \sin 2\theta\langle\tau_x(t)\rangle, \tag{B.6}$$

$$\langle\sigma_x(t)\rangle = \sin 2\theta\langle\tau_z(t)\rangle - \cos 2\theta\langle\tau_x(t)\rangle, \tag{B.7}$$

$$\left\langle\sigma_y(t)\right\rangle = -\left\langle\tau_y(t)\right\rangle. \tag{B.8}$$

By utilizing Eqs. (B.6)–(B.8), the dynamics of the density matrix elements in Eqs. (B.2) and (B.3) can be transformed back into the local basis.

Appendix C. Elements of the matrix M

According to the Liouville operator $\mathcal{D}_i[\rho]$ ($i = E$, B, and C) for the TLS in Eqs. (A.1) and (A.3), the elements of the matrix M in (A.4) are given by

$$M_{11} = 2\gamma_0 \sin^2 2\theta \cos^2 2\theta + \frac{1}{2}\Gamma_B (1 + 2n_B) \sin^2 2\theta \left(\cos^2 2\theta + 1\right) + \frac{1}{2}\Gamma_E (1 + n_E) + \frac{1}{2}\Gamma_C (1 + n_C), \tag{C.1}$$

$$M_{12} = \frac{1}{2}\Gamma_E (1 + 3n_E) - \frac{1}{2}\Gamma_C (1 + 3n_C), \tag{C.2}$$

$$M_{13} = -4\gamma_0 \sin 2\theta \cos^3 2\theta + \Gamma_B (1 + 2n_B) \sin^3 2\theta \cos 2\theta, \tag{C.3}$$

$$M_{14} = -4M_{41} = 2\omega \sin 2\theta, \tag{C.4}$$

$$M_{21} = \frac{1}{2}\Gamma_E (1 + n_E) - \frac{1}{2}\Gamma_C (1 + n_C), \tag{C.5}$$

$$M_{22} = \frac{1}{2}\Gamma_E (1 + 3n_E) + \frac{1}{2}\Gamma_C (1 + 3n_C), \tag{C.6}$$

$$M_{31} = -\gamma_0 \sin 2\theta \cos^3 2\theta + \frac{1}{4}\Gamma_B (1 + 2n_B) \sin^3 2\theta \cos 2\theta, \tag{C.7}$$

$$M_{33} = 2\gamma_0 \cos^4 2\theta + \frac{1}{2}\Gamma_B (1 + 2n_B) \sin^2 2\theta \left(\sin^2 2\theta + 1\right) + \frac{1}{2}\Gamma_E (1 + n_E) + \frac{1}{2}\Gamma_C (1 + n_C), \tag{C.8}$$

$$M_{34} = -M_{43} = -\omega \cos 2\theta, \tag{C.9}$$

$$M_{44} = 2\gamma_0 \cos^2 2\theta + \frac{1}{2}\Gamma_B (1 + 2n_B) \sin^2 2\theta + \frac{1}{2}\Gamma_C (n_C + 1) + \frac{1}{2}\Gamma_E (n_E + 1), \tag{C.10}$$

$$M_{23} = M_{24} = M_{32} = M_{42} = 0. \tag{C.11}$$

References

[1] N. Li, J. Ren, L. Wang, G. Zhang, P. Hänggi, B. Li, Colloquium: Phononics: Manipulating heat flow with electronic analogs and beyond, Rev. Modern Phys. 84 (2012) 1045–1066.
[2] W. Fu, T. Jin, D. He, S. Qu, Effect of dynamical localization on negative differential thermal resistance, Physica A 433 (2015) 211–217.
[3] B. Li, L. Wang, G. Casati, Negative differential thermal resistance and thermal transistor, Appl. Phys. Lett. 88 (2006) 143501.
[4] S. Kumar, Z. Wang, N. Davila, N. Kumari, K.J. Norris, X. Huang, J.P. Strachan, D. Vine, A.L.D. Kilcoyne, Y. Nishi, R.S. Williams, Physical origins of current and temperature controlled negative differential resistances in NbO_2, Nature Commun. 8 (2017) 658.
[5] S. Rolf-Pissarczyk, S. Yan, L. Malavolti, J.A.J. Burgess, G. McMurtrie, S. Loth, Dynamical negative differential resistance in antiferromagnetically coupled few-atom spin chains, Phys. Rev. Lett. 119 (2017) 217201.
[6] A. Zholud, R. Freeman, R. Cao, A. Srivastava, S. Urazhdin, Spin transfer due to quantum magnetization fluctuations, Phys. Rev. Lett. 119 (2017) 257201.
[7] L. Wang, B. Li, Thermal logic gates: Computation with phonons, Phys. Rev. Lett. 99 (2007) 177208.
[8] B. Ai, B. Hu, Heat conduction in deformable Frenkel-Kontorova lattices: Thermal conductivity and negative differential thermal resistance, Phys. Rev. E 83 (2011) 011131.
[9] D. He, B. Ai, H. Chan, B. Hu, Heat conduction in the nonlinear response regime: Scaling, boundary jumps, and negative differential thermal resistance, Phys. Rev. E 81 (2010) 041131.
[10] R. Su, Z. Yuan, J. Wang, Z. Zheng, Interface-facilitated energy transport in coupled Frenkel-Kontorova chains, Front. Phys. 11 (2016) 114401.
[11] R. Su, Z. Yuan, J. Wang, Z. Zheng, Enhanced energy transport owing to nonlinear interface interaction, Sci. Rep. 6 (2016) 19628.
[12] P. Ben-Abdallah, S. Biehs, Near-field thermal transistor, Phys. Rev. Lett. 112 (2014) 044301.
[13] P. Ben-Abdallah, S. Biehs, K. Joulain, Many-body radiative heat transfer theory, Phys. Rev. Lett. 107 (2011) 114301.
[14] K. Joulain, Y. Ezzahri, J. Drevillon, P. Ben-Abdallah, Modulation and amplification of radiative far field heat transfer: Towards a simple radiative thermal transistor, Appl. Phys. Lett. 106 (2015) 133505.
[15] P. Ben-Abdallah, S. Biehs, Phase-change radiative thermal diode, Appl. Phys. Lett. 103 (2013) 191907.
[16] K. Joulain, J. Drevillon, Y. Ezzahri, J. Ordonez-Miranda, Quantum thermal transistor, Phys. Rev. Lett. 116 (2016) 200601.
[17] Y. Zhang, Z. Yang, X. Zhang, B. Lin, G. Lin, J. Chen, Coulomb-coupled quantum-dot thermal transistors, Europhys. Lett. 122 (2018) 17002.
[18] R. Sánchez, H. Thierschmann, L.W. Molenkamp, All-thermal transistor based on stochastic switching, Phys. Rev. B 95 (2017) 241401(R).
[19] R. Alicki, D. Gelbwaser-Klimovsky, A. Jenkins, A thermodynamic cycle for the solar cell, Ann. Phys. 378 (2017) 71–87.

[20] H. Li, Y. Wang, H. Hao, S. Liu, J. Ding, Performance optimization and parameter design of a benzene molecule heat engine, Physica A 513 (2019) 798–807.
[21] K.E. Dorfman, D. Xu, J. Cao, Efficiency at maximum power of a laser quantum heat engine enhanced by noise-induced coherence, Phys. Rev. E 97 (2018) 042120.
[22] E. Romero, V.I. Novoderezhkin, R. van Grondelle, Quantum design of photosynthesis for bio-inspired solar-energy conversion, Nature 543 (2017) 355–365.
[23] A. Fruchtman, R. Gómez-Bombarelli, B.W. Lovett, E.M. Gauger, Photocell optimization using dark state protection, Phys. Rev. Lett. 117 (2016) 203603.
[24] S. Su, C. Sun, S. Li, J. Chen, Photoelectric converters with quantum coherence, Phys. Rev. E 93 (2016) 052103.
[25] S.W. Li, C.Y. Cai, C.P. Sun, Steady quantum coherence in non-equilibrium environment, Ann. Phys. 360 (2015) 19–32.
[26] E. Romero, R. Augulis, V.I. Novoderezhkin, M. Ferretti, J. Thieme, D. Zigmantas, R. van Grondelle, Quantum coherence in photosynthesis for efficient solar-energy conversion, Nat. Phys. 10 (2014) 676–682.
[27] J. Brédas, E.H. Sargent, G.D. Scholes, Photovoltaic concepts inspired by coherence effects in photosynthetic systems, Nature Mater. 16 (2017) 35–44.
[28] H.E.D. Scovil, E.O. Schulz-DuBois, Three-level masers as heat engines, Phys. Rev. Lett. 2 (1959) 262–263.
[29] E. Boukobza, D.J. Tannor, Three-level systems as amplifiers and attenuators: A thermodynamic analysis, Phys. Rev. Lett. 98 (2007) 240601.
[30] D. Xu, C. Wang, Y. Zhao, J. Cao, Polaron effects on the performance of light-harvesting systems: A quantum heat engine perspective, New J. Phys. 18 (2016) 023003.
[31] N. Lambert, Y.N. Chen, Y.C. Cheng, C.M. Li, G.Y. Chen, F. Nori, Quantum biology, Nat. Phys. 9 (2013) 10–18.
[32] T. Werlang, D. Valente, Heat transport between two pure-dephasing reservoirs, Phys. Rev. E 91 (2015) 012143.
[33] G.D. Mahan, Many-Particle Physics, Plenum Press, New York, 1993.
[34] M.R. Delbecq, L.E. Bruhat, J.J. Viennot, S. Datta, A. Cottet, T. Kontos, Photon-mediated interaction between distant quantum dot circuits, Nature Commun. 4 (2013) 1400.
[35] E. Rozbicki, P. Machnikowski, Quantum kinetic theory of phonon-assisted excitation transfer in quantum dot molecules, Phys. Rev. Lett. 100 (2008) 027401.
[36] C. Wang, J. Ren, J. Cao, Nonequilibrium energy transfer at nanoscale: A unified theory from weak to strong coupling, Sci. Rep. 5 (2015) 11787.
[37] D. Xu, K. Schulten, Coupling of protein motion to electron transfer in a photosynthetic reaction center: Investigating the low temperature behavior in the framework of the spin-boson model, Chem. Phys. 182 (1994) 91–117.
[38] D. Xu, J. Cao, Non-canonical distribution and non-equilibrium transport beyond weak system-bath coupling regime: A polaron transformation approach, Front. Phys. 11 (2016) 110308.
[39] H.P. Breuer, F. Petruccione, The Theory of Open Quantum Systems, Oxford University Press, Oxford, 2001.
[40] E. Boukobza, D.J. Tannor, Thermodynamic analysis of quantum light amplification, Phys. Rev. A 74 (2006) 063822.
[41] E. Boukobza, D.J. Tannor, Thermodynamics of bipartite systems: Application to light-matter interactions, Phys. Rev. A 74 (2006) 063823.
[42] R. Kosloff, A. Levy, Quantum heat engines and refrigerators: Continuous devices, Annu. Rev. Phys. Chem. 65 (2014) 365–393.
[43] M. Orszag, Quantum Optics: Including Noise Reduction, Trapped Ions, Quantum Trajectories, and Decoherence, Springer, Switzerland, 2016.
[44] P.P. Hofer, J.B. Brask, M. Perarnau-Llobet, N. Brunner, Quantum thermal machine as a thermometer, Phys. Rev. Lett. 119 (2017) 090603.
[45] J.X. Wang, H. Dong, S.W. Li, Magnetic dipole–dipole interaction induced by the electromagnetic field, Phys. Rev. A 97 (2018) 013819.
[46] P. Kirton, J. Keeling, Suppressing and restoring the dicke superradiance transition by dephasing and decay, Phys. Rev. Lett. 118 (2017) 123602.
[47] E. Bauch, C.A. Hart, J.M. Schloss, M.J. Turner, J.F. Barry, P. Kehayias, S. Singh, R.L. Walsworth, Ultralong dephasing times in solid-state spin ensembles via quantum control, Phys. Rev. X 8 (2018) 031025.
[48] M.C. Kuzyk, H. Wang, Scaling phononic quantum networks of solid-state spins with closed mechanical subsystems, Phys. Rev. X 8 (2018) 041027.
[49] M. Qin, H.Z. Shen, X.L. Zhao, X.X. Yi, Effects of system-bath coupling on a photosynthetic heat engine: A polaron master-equation approach, Phys. Rev. A 96 (2017) 012125.
[50] K.E. Dorfman, D.V. Voronine, S. Mukamel, M.O. Scully, Photosynthetic reaction center as a quantum heat engine, Proc. Natl. Acad. Sci. USA 110 (2013) 2746–2751.
[51] M.O. Scully, K.R. Chapin, K.E. Dorfman, M.B. Kim, A. Svidzinsky, Quantum heat engine power can be increased by noise-induced coherence, Proc. Natl. Acad. Sci. USA 108 (2011) 15097–15100.